Discrete-Time Sliding Mode with Time Delay Estimation of a Six-Phase Induction Motor Drive

Y. Kali[1], J. Rodas[2], M. Ayala[2], M. Saad[1], R. Gregor[2], K. Benjelloun[3], J. Doval-Gandoy[4] and G. Goodwin[5]
[1]École de Technologie Supérieure, Quebec University, Montreal, QC H3C 1K3, Canada (y.kali88@gmail.com)
[2]Laboratory of Power and Control Systems, Facultad de Ingeniería, Universidad Nacional de Asunción, Paraguay
[3]Engineering School, École Mohammadia d'Ingénieurs, University of Mohammed V, Rabat, Morocco
[4]Applied Power Electronics Technology Research Group, Universidad de Vigo, Spain
[5]School of Electrical Engineering and Computer Science, University of Newcastle, Australia

***Abstract*—This paper investigates the problem of stator current control in presence of uncertainties and unmeasurable rotor current for a six-phase induction motor drive. An inner control loop based on a robust discrete-time sliding mode with time delay estimation method is proposed to ensure the finite-time convergence of the stator currents to their desired references while the proportional-integral controller is used for the outer speed control. Sufficient conditions are established to ensure the stability of the closed-loop system. Simulation results were carried out to verify the performance of the proposed robust control strategy for a six-phase induction motor drive.**

***Index Terms*—Discrete-time sliding mode, time delay estimation, multiphase induction machine, speed control, current control, field oriented control.**

I. Introduction

Multiphase drives have received a great interests from power electronics community due to their good features in comparison with the traditional three-phase drives such as lower current/power per phase and lower torque ripple and fault tolerant capabilities without adding extra hardware [1]–[3]. Nowadays, they are extensively used for high-power and reliable applications such as wind energy generation systems and electric vehicles [3], [4]. Most of the control strategies applied for multiphase drives are an extension of the three-phase case such as proportional-integral pulse-width modulation, proportional-resonant finite-control-set model predictive control, predictive torque control, direct torque control, sensorless, among others [5]–[12]. Recent works also extends the above-mentioned techniques to the post-fault operation [13]–[16]. However, little attention has been paid to robust nonlinear controllers based on fuzzy logic and/or sliding mode control (SMC) strategies [17]–[20].

Indeed, SMC is one of the robust proposed nonlinear control techniques in literature. The aim of this technique is to force the system trajectories to converge to a user-chosen switching surface [21] in finite-time even in presence of uncertainties and disturbances using discontinuous controller. However, to ensure high performances, the switching gains should be chosen as large as possible to reject the effect of the bounded uncertainties. Therefore, this choice causes the major drawback of SMC, the well-known chattering phenomenon [22], [23]. This phenomenon has a negative impact on the system actuators which can lead to the deterioration of the controlled system and/or the instability. To solve this problem, many developments have been published, we cite in this context:

- Sliding mode based on a boundary layer [24]. The idea consists on using continuous functions such as saturation instead the signum function. This proposition allows chattering reduction, but the finite-time convergence is not guaranteed anymore which is very desirable while critical convergence time is required.
- Observer-based sliding mode control [25], [26]. This method reduces the problem of designing a robust controller into the problem of designing a robust observer. It means that if the uncertainties estimation is not exact, the desired performances will be affected.
- Higher order sliding mode (HOSM) [27]–[29]. The basic idea is to make the discontinuous term acting on the first time derivative of the control input, then, by integrating the control input becomes continuous. This approach reduces the chattering phenomenon and allows higher precision. However, the required informations (first time derivative of the selected sliding surface) are increased which make the implementation difficult.

Recently, a promising idea that consists on combining sliding mode control with time delay estimation (TDE) method for uncertain nonlinear systems [30], [31]. The proposed method has been successfully tested on a redundant robot arm. The basic idea is to estimate matched uncertainties that are assumed to be Lipschitz using delayed states and inputs informations. Then, the estimated terms are added in the equivalent controller in order to allow a small choice of the switching gains of the discontinuous controller.

Nevertheless, the real time implementation is generally performed through discrete systems [32]. For this reason, the development of the controller should be done in discrete time. Therefore, it is suitable to use the six-phase IM model in discrete time representation during the design procedure because the inherent properties of the sliding mode method might not be maintained after discretization.

Therefore, in this paper, a discrete-time sliding mode control (DSMC) with TDE method is proposed for the inner current control loop of a rotor field oriented control (RFOC) of a six-phase induction motor (IM) drive. The rest of the paper

is organized as follows. Section II presents the mathematical model of the system while controller design is explained in Section III. Simulation results are provided in Section IV. Section V draws some conclusions.

II. Six-phase IM and VSI model

The analyzed system consists of an asymmetrical six-phase IM fed by two 2-level (2L) VSI shown in Fig. 1. After using the vector space decomposition (VSD) approach, the decoupling transformation $\mathbf{T}$ gives $\alpha - \beta$ subspace which is related to flux/torque producing components and loss-producing $x - y$ subspace and a zero-sequence subspace. In the rest of this paper, matrices and vectors will be denoted by capital and small bold-face letters, respectively. Then, by using an amplitude invariant criterion, $\mathbf{T}$ is defined as follows:

$$\mathbf{T} = \frac{1}{3}\begin{bmatrix} 1 & \frac{\sqrt{3}}{2} & -\frac{1}{2} & -\frac{\sqrt{3}}{2} & -\frac{1}{2} & 0 \\ 0 & \frac{1}{2} & \frac{\sqrt{3}}{2} & \frac{1}{2} & -\frac{\sqrt{3}}{2} & -1 \\ 1 & -\frac{\sqrt{3}}{2} & -\frac{1}{2} & \frac{\sqrt{3}}{2} & -\frac{1}{2} & 0 \\ 0 & \frac{1}{2} & -\frac{\sqrt{3}}{2} & \frac{1}{2} & \frac{\sqrt{3}}{2} & -1 \\ 1 & 0 & 1 & 0 & 1 & 0 \\ 0 & 1 & 0 & 1 & 0 & 1 \end{bmatrix} \tag{1}$$

The discrete model of the system in state-space representation is represented by the following equations [7]:

$$\mathbf{x}_1(k+1) = \mathbf{A}_1\,\mathbf{x}_1(k) + \mathbf{H}_1\,\mathbf{x}_3(k) + \mathbf{B}_1\,\mathbf{u}_1(k) + \mathbf{n}_1(k) \tag{2}$$
$$\mathbf{x}_2(k+1) = \mathbf{A}_2\,\mathbf{x}_2(k) + \mathbf{B}_2\,\mathbf{u}_2(k) + \mathbf{n}_2(k) \tag{3}$$
$$\mathbf{x}_3(k+1) = \mathbf{A}_3\,\mathbf{x}_1(k) + \mathbf{H}_2\,\mathbf{x}_3(k) + \mathbf{B}_3\,\mathbf{u}_1(k) + \mathbf{n}_3(k) \tag{4}$$
$$\mathbf{y}(k) = \mathbf{C}\,\mathbf{x}(k) \tag{5}$$

being the stator and rotor currents state vector:

$$\mathbf{x}(k) = [\mathbf{x}_1(k),\, \mathbf{x}_2(k),\, \mathbf{x}_3(k)]^T \tag{6}$$

with:

$$\mathbf{x}_1(k) = [i_{s\alpha}(k),\, i_{s\beta}(k)]^T \tag{7}$$
$$\mathbf{x}_2(k) = [i_{sx}(k),\, i_{sy}(k)]^T \tag{8}$$
$$\mathbf{x}_3(k) = [i_{r\alpha}(k),\, i_{r\beta}(k)]^T \tag{9}$$

while the stator voltages represents the input vectors:

$$\mathbf{u}_1(k) = [u_{s\alpha}(k),\, u_{s\beta}(k)]^T \tag{10}$$
$$\mathbf{u}_2(k) = [u_{sx}(k),\, u_{sy}(k)]^T \tag{11}$$

and the stator currents the output vector:

$$\mathbf{y}(k) = [\mathbf{x}_1(k),\, \mathbf{x}_2(k)]^T \tag{12}$$
$$= [i_{s\alpha}(k),\, i_{s\beta}(k),\, i_{sx}(k),\, i_{sy}(k)]^T \tag{13}$$

and $\mathbf{n}_i(k) \in R^2$ for $i = 1, 2, 3$ denote the uncertain vectors. The stator voltages have a discrete nature due to the VSI model and the relationship between them is represented as:

$$[u_{s\alpha}(k),\, u_{s\beta}(k),\, u_{sx}(k),\, u_{sy}(k)]^T = V_{\rm dc}\,\mathbf{T}\,\mathbf{M} \tag{14}$$

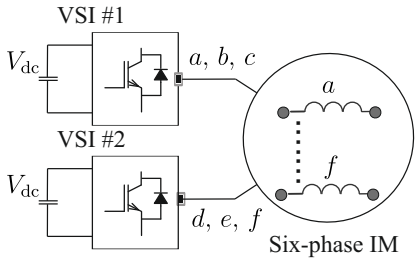

Fig. 1. Scheme of the six-phase IM drive.

where the gating signals are $\mathbf{S} = [S_a,\, S_b,\, S_c,\, S_d,\, S_e,\, S_f]$, being $S_i \in \{0,\, 1\}$, $V_{\rm dc}$ is the DC-bus voltage and the VSI model is:

$$\mathbf{M} = \frac{1}{3}\begin{bmatrix} 2 & 0 & -1 & 0 & -1 & 0 \\ 0 & 2 & 0 & -1 & 0 & -1 \\ -1 & 0 & 2 & 0 & -1 & 0 \\ 0 & -1 & 0 & 2 & 0 & -1 \\ -1 & 0 & -1 & 0 & 2 & 0 \\ 0 & -1 & 0 & -1 & 0 & 2 \end{bmatrix}\mathbf{S}^T. \tag{15}$$

The matrices $\mathbf{A}_1$, $\mathbf{A}_2$, $\mathbf{A}_3$, $\mathbf{H}_1$, $\mathbf{H}_2$, $\mathbf{B}_1$, $\mathbf{B}_2$ and $\mathbf{B}_3$ are defined as follows:

$$\mathbf{A}_1 = \begin{bmatrix} a_{11} & a_{12} \\ a_{21} & a_{22} \end{bmatrix},\ \mathbf{A}_2 = \begin{bmatrix} a_{33} & 0 \\ 0 & a_{44} \end{bmatrix},\ \mathbf{A}_3 = \begin{bmatrix} a_{51} & a_{52} \\ a_{61} & a_{62} \end{bmatrix}$$

$$\mathbf{H}_1 = \begin{bmatrix} h_{11} & h_{12} \\ h_{21} & h_{22} \end{bmatrix},\ \mathbf{H}_2 = \begin{bmatrix} h_{31} & h_{32} \\ h_{41} & h_{42} \end{bmatrix}$$

$$\mathbf{B}_1 = \begin{bmatrix} b_1 & 0 \\ 0 & b_1 \end{bmatrix},\ \mathbf{B}_2 = \begin{bmatrix} b_2 & 0 \\ 0 & b_2 \end{bmatrix},\ \mathbf{B}_3 = \begin{bmatrix} b_3 & 0 \\ 0 & b_3 \end{bmatrix}$$

where:

$a_{11} = a_{22} = 1 - T_s\,c_2\,R_s$ — $a_{12} = -a_{21} = T_s\,c_4 L_m\,\omega_{r(k)}$
$h_{11} = h_{22} = T_s\,c_4\,R_r$ — $h_{12} = -h_{21} = T_s\,c_4 L_r\,\omega_{r(k)}$
$a_{33} = a_{44} = 1 - T_s\,c_3\,R_s$ — $a_{51} = a_{62} = -T_s\,c_4\,R_s$
$a_{52} = -a_{61} = -T_s\,c_5\,L_m\,\omega_{r(k)}$ — $h_{31} = h_{42} = 1 - T_s\,c_5\,R_r$
$h_{32} = -h_{41} = -c_5\,\omega_{r(k)}\,T_s\,L_r$ — $b_1 = T_s\,c_2$
$b_2 = T_s\,c_3$ — $b_3 = -T_s\,c_4$

being T_s the sampling time and c_1 to c_5 are defined as: $c_1 = L_s L_r - L_m^2$, $c_2 = \frac{L_r}{c_1}$, $c_3 = \frac{1}{L_{ls}}$ $c_4 = \frac{L_m}{c_1}$ $c_5 = \frac{L_s}{c_1}$. The electrical parameters of the systems are R_s, R_r, $L_r = L_{lr} + L_m$, $L_s = L_{ls} + L_m$, L_r and L_m. The rotor electrical speed (ω_r) has a relationship with load torque (T_l) and generated torque (T_e) as follows:

$$J_m\,\dot{\omega}_r + B_m\,\omega_r = P\,(T_e - T_l) \tag{16}$$

being B_m and J_m the friction and the inertia coefficient, respectively, P the number of pole pairs and T_e is:

$$T_e = 3\,P\,M\,(i_{r\beta}\,i_{s\alpha} - i_{r\alpha}\,i_{s\beta}) \tag{17}$$

where M is the magnetizing inductance.

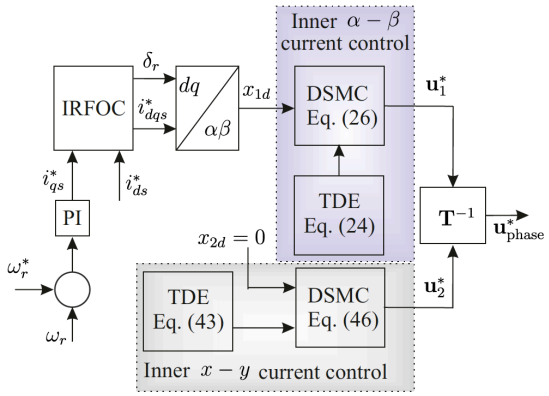

Fig. 2. Block diagram of the proposed speed control based on IRFOC technique and the DSMC with TDE method for the inner current control.

III. Proposed Controller

A. Outer Control Loop

The aim of the outer loop is to control the speed. To that end, a PI controller with a saturation is used due to its simplicity. For the outer loop, the PI speed controller is selected to obtain the dynamic reference current $i^*_{qs}(k)$. Then, the process of the slip frequency ($\omega_{sl}(k)$) estimation is executed in the same way as the indirect RFOC methods, from the reference currents ($i^*_{ds}(k), i^*_{qs}(k)$) in the dynamic reference frame and the electrical parameters of the six-phase IM.

B. Inner Control Loop

The aim of the inner loop is to control the stator currents. To that end, the DSMC with TDE method will be designed to force the stator current in the $\alpha-\beta$ and the $x-y$ sub-spaces to converge to their desired references in finite-time with high accuracy even in presence of unmeasurable states (i,e. rotor currents) and uncertainties.

1) Control of Stator Current in $\alpha-\beta$ Sub-Space: To quantify the control objective, let $\mathbf{x}^d_1(k) = i^*_{s\phi}(k) \in R^2$ to be the desired reference with $\phi \in \{\alpha, \beta\}$ and $e_\phi(k) = \mathbf{x}_1(k) - \mathbf{x}^d_1(k) = i_{s\phi}(k) - i^*_{s\phi}(k) \in R^2$ be the tracking error. Now, let us select the sliding surface [21] to be the error variable as:

$$\sigma(k) = e_\phi(k) \tag{18}$$

To ensure ideal sliding motion, the following conditions must be verified:

$$\sigma(k) = 0,\ \sigma(k+1) = 0 \tag{19}$$

where $\sigma(k+1)$ is obtained as:

$$\begin{aligned}\sigma(k+1) = e_\phi(k+1) &= \mathbf{x}_1(k+1) - \mathbf{x}^d_1(k+1)\\ &= \mathbf{A}_1\,\mathbf{x}_1(k) + \mathbf{H}_1\,\mathbf{x}_3(k) + \mathbf{B}_1\,\mathbf{u}_1(k)\\ &\quad + \mathbf{n}_1(k) - \mathbf{x}^d_1(k+1)\end{aligned} \tag{20}$$

As the classical sliding motion is not enough to ensure robustness, the following reaching law is chosen:

$$\sigma(k+1) = \lambda\,\sigma(k) - T_s\rho\,\text{sign}(\sigma(k)) \tag{21}$$

where $\lambda = \text{diag}(\lambda_1, \lambda_2)$ with $0 < \lambda_i < 1$ for $i = 1, 2$, $\rho \in R^{2\times 2}$ is a diagonal positive matrix and $\text{sign}(\sigma(k)) = [\text{sign}(\sigma_1(k)), \text{sign}(\sigma_2(k))]^T$ with:

$$\text{sign}(\sigma_i(k)) = \begin{cases} 1, & \text{if } \sigma_i(k) > 0\\ 0, & \text{if } \sigma_i(k) = 0\\ -1, & \text{if } \sigma_i(k) < 0\end{cases} \tag{22}$$

Hence, the DSMC law for the stator current in $\alpha-\beta$ sub-space described in (2) is obtained as:

$$\begin{aligned}\mathbf{u}_1(k) = -\mathbf{B}_1^{-1}\,[&\mathbf{A}_1\mathbf{x}_1(k) - \mathbf{x}^d_1(k+1) - \lambda\,\sigma(k)\cdots\\ &\cdots + \mathbf{H}_1\mathbf{x}_3(k) + \mathbf{n}_1(k) + T_s\rho\,\text{sign}(\sigma(k))]\end{aligned} \tag{23}$$

As the rotor currents $\mathbf{x}_3(k)$ are not measurable and as $\mathbf{n}_1(k)$ is unknown, the control performance might not be satisfactory. Then, assuming that $\mathbf{x}_3(k)$ and $\mathbf{n}_1(k)$ do not vary largely between two consecutive sampling time and based on (2), they can be estimated using TDE [28], [33] method as:

$$\begin{aligned}\mathbf{H}_1\hat{\mathbf{x}}_3(k) + \hat{\mathbf{n}}_1(k) &\cong \mathbf{H}_1\mathbf{x}_3(k-1) + \mathbf{n}_1(k-1)\\ &= \mathbf{x}_1(k) - \mathbf{A}_1\mathbf{x}_1(k-1) - \mathbf{B}_1\mathbf{u}_1(k-1)\end{aligned} \tag{24}$$

Definition 3.1: For a discrete system, a quasi sliding mode is considered in the vicinity of the sliding surface, such that $|\sigma(k)| < \varepsilon$, with ε is a positive constant called the quasi-sliding-mode band width. To guarantee a convergent quasi sliding mode, the following sufficient and necessary conditions given in [28], [34] must be verified for $i = 1, 2$:

$$\begin{cases}\sigma_i(k) > \varepsilon \Rightarrow -\varepsilon \le \sigma_i(k+1) < \sigma_i(k)\\ \sigma_i(k) < -\varepsilon \Rightarrow \sigma_i(k) < \sigma_i(k+1) \le \varepsilon\\ |\sigma_i(k)| \le \varepsilon \Rightarrow |\sigma_i(k+1)| \le \varepsilon\end{cases} \tag{25}$$

Theorem 3.1: The DSMC with TDE method for the stator current in the $\alpha-\beta$ sub-space given in (2) is given by:

$$\begin{aligned}\mathbf{u}_1(k) = \mathbf{B}_1^{-1}\,[&\mathbf{x}_{1d}(k+1) - \mathbf{A}_1\mathbf{x}_1(k) - \mathbf{H}_1\hat{\mathbf{x}}_3(k)\cdots\\ &\cdots - \hat{\mathbf{n}}_1(k) + \lambda\,\sigma(k) - T_s\rho\,\text{sign}(\sigma(k))]\end{aligned} \tag{26}$$

ensures a quasi sliding mode if the following condition is met:

$$\rho_i > \frac{1}{T_s}\delta_i \quad for\ i = 1, 2 \tag{27}$$

Proof. Substituting the calculated discrete-time controller (13) in equation (9) leads to:

$$\sigma(k+1) = E + \lambda\,\sigma(k) - T_s\rho\,\text{sign}(\sigma(k)) \tag{28}$$

where $E = \mathbf{H}_1\,(\mathbf{x}_3(k) - \hat{\mathbf{x}}_3(k)) + (\mathbf{n}_1(k) - \hat{\mathbf{n}}_1(k))$ is the bounded TDE error such as for $i = 1, 2$:

$$|E_i| < \delta_i \tag{29}$$

Now, let us choose $\varepsilon = T_s\rho_i + \delta_i$. Hence, equation (25) can be rewritten as:

$$\begin{aligned}&\sigma_i(k) > T_s\rho_i + \delta_i \Rightarrow -T_s\rho_i - \delta_i \le \sigma_i(k+1) < \sigma_i(k)\\ &\sigma_i(k) < -T_s\rho_i - \delta_i \Rightarrow \sigma_i(k) < \sigma_i(k+1) \le T_s\rho_i + \delta_i\\ &|\sigma_i(k)| \le T_s\rho_i + \delta_i \Rightarrow |\sigma_i(k+1)| \le T_s\rho_i + \delta_i\end{aligned} \tag{30}$$

1. Consider the first case where $\sigma_i(k) > T_s\rho_i + \delta_i$, then $\sigma_i(k) > 0$, $\text{sign}(\sigma_i(k)) = 1$ and:

$$\begin{aligned} \sigma_i(k+1) &= E_i + \lambda_i\, \sigma_i(k) - T_s\rho_i \\ \sigma_i(k+1) - \sigma_i(k) &= E_i + (\lambda_i - 1)\, \sigma_i(k) - T_s\rho_i \end{aligned} \tag{31}$$

Since the condition in (27) is verified, then $\sigma_i(k+1) - \sigma_i(k) < 0 \Rightarrow \sigma_i(k+1) < \sigma_i(k)$.
In addition, $-T_s\rho_i - \delta_i \leq \sigma_i(k+1)$ can be written as:

$$E_i + \lambda_i\, \sigma_i(k) - T_s\rho_i \geq -T_s\rho_i - \delta_i \tag{32}$$

Hence:

$$\sigma_i(k) \geq \frac{1}{\lambda_i}(E_i - \delta_i) \tag{33}$$

which is is always true since $\sigma_i(k) > 0$ and $(E_i - \delta_i) < 0$.
2. Consider the second case where $\sigma_i(k) < -T_s\rho_i - \delta_i$, which means that $\sigma_i(k) < 0$ and $\text{sign}(\sigma_i(k)) = -1$. Then, $\sigma_i(k) < \sigma_i(k+1)$ can be rewritten as:

$$\begin{aligned} \sigma_i(k) &< E_i + \lambda_i\, \sigma_i(k) + T_s\rho_i \\ (1 - \lambda_i)\, \sigma_i(k) &< E_i + T_s\rho_i \end{aligned} \tag{34}$$

which is always true since the condition (27) is verified. Moreover, $\sigma_i(k+1) < T_s\rho_i + \delta_i$ can be rewritten as:

$$E_i + \lambda_i\, \sigma_i(k) + T_s\rho_i < T_s\rho_i + \delta_i \tag{35}$$

It is obvious that the above inequality is always true since $\sigma_i(k) < 0$ and $\delta_i > E_i$.
3. Consider the third case where $|\sigma_i(k)| \leq \varepsilon$, then:
   a. if $\sigma_i(k) > 0$, then $|\sigma_i(k)| \leq \varepsilon$ becomes:

$$0 < \sigma_i(k) < \varepsilon \tag{36}$$

   Multiplying by λ_i and adding $E_i - T_s\rho_i$ to all the parts of the above equation leads to:

$$\begin{aligned} E_i - T_s\rho_i < \sigma_i(k+1) &< E_i - T_s\rho_i + \lambda_i\, \varepsilon \\ -\varepsilon < \sigma_i(k+1) &< \varepsilon \\ |\sigma_i(k+1)| &\leq \varepsilon \end{aligned} \tag{37}$$

   b. if $\sigma_i(k) < 0$, then $|\sigma_i(k)| \leq \varepsilon$ becomes:

$$-\varepsilon < \sigma_i(k) < 0 \tag{38}$$

   Once again, multiplying by λ_i and adding $E_i + T_s\rho_i$ to all the parts of (38) gives:

$$\begin{aligned} E_i + T_s\rho_i - \lambda_i\, \varepsilon < \sigma_i(k+1) &< E_i + T_s\rho_i \\ -\varepsilon < \sigma_i(k+1) &< \varepsilon \\ |\sigma_i(k+1)| &\leq \varepsilon \end{aligned} \tag{39}$$

Hence:

$$|\sigma_i(k+1)| < \varepsilon = T_s\rho_i + \delta_i \tag{40}$$

The conditions in (30) being verified, the existence of the convergent quasi sliding mode is proved. Therefore, the proposed discrete-time controller in (13) is stable.
This concludes the proof.

2) Control of Stator Current in $x - y$ Sub-Space: The complete study of DSMC with TDE is described in the previous part. To control the stator current in the $x - y$ sub-space, the same methodology will be used. The sliding surface here is selected as:

$$\sigma^*(k) = e_{s_{xy}}(k) = \mathbf{x}_2(k) - \mathbf{x}_2^d(k) \tag{41}$$

where $\mathbf{x}_2^d(k) = [i_{sx}^*(k),\ i_{sy}^*(k)]^T$ denotes the desired currents and $e_{s_{xy}}(k)$ represents the tracking error variable. Therefore, $\sigma^*(k+1)$ is calculated as follows:

$$\begin{aligned} \sigma^*(k+1) = e_{s_{xy}}(k+1) &= \mathbf{x}_2(k+1) - \mathbf{x}_2^d(k+1) \\ &= \mathbf{A}_2\, \mathbf{x}_2(k) + \mathbf{B}_2\, \mathbf{u}_2(k) + \mathbf{n}_2(k) - \mathbf{x}_2^d(k+1) \end{aligned} \tag{42}$$

Finally, the discrete-time controller is obtained by substituting the uncertain vector $\mathbf{n}_2(k)$ by its estimate using TDE method:

$$\begin{aligned} \hat{\mathbf{n}}_2(k) &\cong \mathbf{n}_2(k-1) \\ &= \mathbf{x}_2(k) - \mathbf{A}_2\, \mathbf{x}_2(k-1) - \mathbf{B}_2\, \mathbf{u}_2(k-1) \end{aligned} \tag{43}$$

and by resolving:

$$\sigma^*(k+1) = \Gamma\, \sigma^*(k) - T_s\varrho\, \text{sign}(\sigma^*(k)) \tag{44}$$

where $\Gamma = \text{diag}(\Gamma_1, \Gamma_2)$ with $0 < \Gamma_i < 1$ for $i = 1, 2$, $\varrho \in R^{2\times 2}$ is a diagonal positive matrix and $\text{sign}(\sigma^*(k)) = [\text{sign}(\sigma_1^*(k)), \text{sign}(\sigma_2^*(k))]^T$.

Theorem 3.2: If the controller gains are chosen for $i = 1, 2$ as follows:

$$\varrho_i > \frac{1}{T_s}\delta_i^* \tag{45}$$

with $\delta_i^* > 0$ is the upper-bound of the TDE error $E^* = \mathbf{n}_2(k) - \mathbf{n}_2(k-1)$. Then, the following DSMC with TDE method for the stator current in the $x-y$ sub-space (3) ensures a quasi sliding motion:

$$\begin{aligned} \mathbf{u}_2(k) = \mathbf{B}_2^{-1} [\mathbf{x}_{2d}(k+1) - \mathbf{A}_2\mathbf{x}_2(k) - \hat{\mathbf{n}}_2(k) \cdots \\ \cdots + \Gamma\, \sigma^*(k) - T_s\varrho\, \text{sign}(\sigma^*(k))] \end{aligned} \tag{46}$$

Proof. The stability analysis is similar to the one described for the stator currents in $\alpha - \beta$ sub-space.

IV. Numerical Simulation

A MATLAB/Simulink simulation program has been designed for a six-phase IM in order to prove the effectiveness of the proposed method. Numerical integration using first order Euler's discretization method has been applied to compute the evolution of the state space variables in the time domain. The electrical and mechanical parameters of the six-phase IM are detailed in Table I.

In this simulation, a sampling frequency of 10 kHz, a torque load of 2 Nm connected to the six-phase IM and a fixed d current ($i_{ds}^* = 1$ A) have been used. The PI gains are chosen to be $K_p = 9.17$ and $K_I = 0.027$.

In addition, the gains of the DSMC with TDE used for stator currents tracking in $\alpha - \beta$ sub-space are:

$$\lambda = \text{diag}(0.5, 0.5),\ \rho_1 = \rho_2 = 30$$

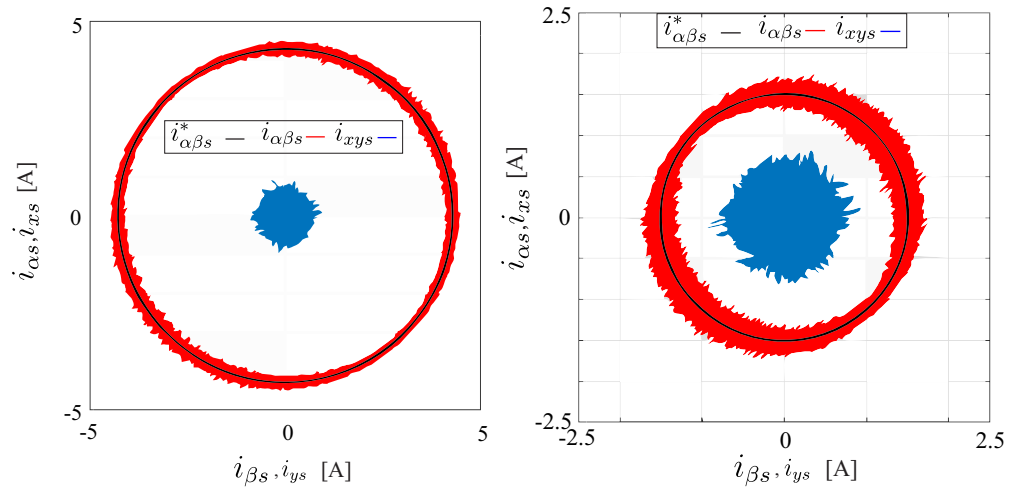

Fig. 3. Stator currents in $\alpha - \beta$ and $x - y$ sub-spaces for a sampling frequency of 10 kHz: (a) Amplitude of 4.5 A; (b) Amplitude of 1.5 A.

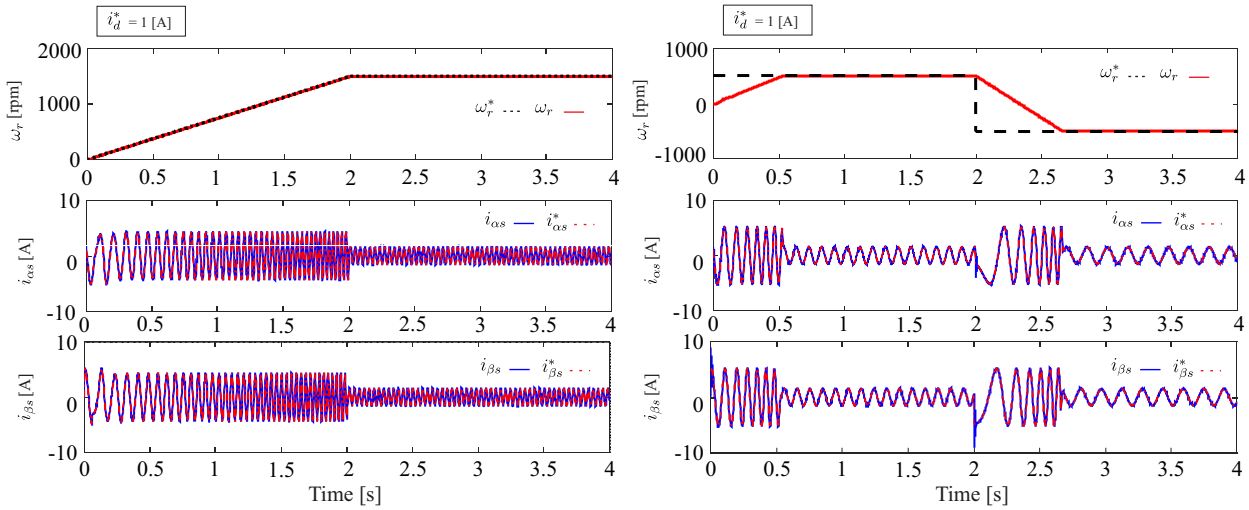

Fig. 4. Stator currents in $\alpha - \beta$ sub-space for transient and steady-state rotor speed for a sampling frequency of 10 kHz: (a) 1500 rpm of steady state response; (b) Reversal condition of 500 to -500 rpm.

While the gains of the DSMC with TDE used for stator currents tracking in $x - y$ sub-space are:

$$\Gamma = \text{diag}(0.9, 0.9), \;\; \varrho_1 = \varrho_2 = 30$$

The behavior of the stator currents in the $\alpha - \beta$ and $x - y$ sub-spaces are shown in Fig. 3(a) and Fig. 3(b) for different $i^d_{\alpha\beta s}$ amplitudes. Fig. 4(a) exposes the stator currents evolution in $\alpha - \beta$ sub-space for a transient and steady-state rotor speed reference and Fig. 4(b) demonstrates the stator currents behavior for a reversal condition where the rotor speed reference changes from 500 to -500 rpm. The proposed controllers ensure high accuracy tracking of the system currents to their desired references in a finite-time.

TABLE I
ELECTRICAL AND MECHANICAL PARAMETERS OF THE SIX-PHASE IM

R_r	6.9 Ω	L_s	654.4 mH
R_s	6.7 Ω	P	1
L_{ls}	5.3 mH	B_i	0.0004 kg.m^2/s
L_{lr}	12.8 mH	J_i	0.07 kg.m^2
L_r	626.8 mH	Nominal Power	2 kW
L_m	614 mH	Nominal Speed	3000 rpm

To quantify the speed and currents tracking, the mean square error (MSE) and total harmonic distortion (THD) are used as figures of merit. For a 500 rpm of speed rotor reference, the proposed controller obtains a MSE of 1.1460 rpm, 0.0550 A and 0.1640 A for the measured speed, $\alpha-\beta$ and $x-y$ currents respectively. For a 1500 rpm of speed rotor reference, the proposed controller shows a MSE of 1.1457 rpm, 0.0575 A

and 0.1860 A for the measured speed, $\alpha-\beta$ and $x-y$ currents respectively. As for the THD analysis, for 500 and 1500 rpm of speed reference, it is obtained 5.3 % and 5.6 % for $\alpha-\beta$ currents respectively.

V. Conclusion

In this paper, a speed control based on RFOC strategy with an inner DSMC with TDE stator currents control is proposed. The proposed method is based on TDE method that estimates effectively and simply the unmeasurable rotor currents, uncertainties and disturbances and on DSMC that provides robustness against TDE error, finite-time convergence and chattering reduction. The efficiency of the proposed DSMC with TDE is confirmed by numerical simulations on a six-phase IM drive. The proposed controller provides excellent performances in steady state as well as in dynamic process. Furthermore, the average switching frequency of the proposed method is even lower than the conventional SMC and other controllers. Further research will be initiated for real-time implementation.

Acknowledgment

The authors wish to thank the financial support from the Paraguayan Science and Technology National Council (CONACYT) through project 14-INV-101.

References

[1] F. Barrero and M. J. Duran, "Recent advances in the design, modeling, and control of multiphase machines: Part I," *IEEE Trans. Ind. Electron.*, vol. 63, no. 1, pp. 449–458, 2016.

[2] M. J. Duran and F. Barrero, "Recent advances in the design, modeling, and control of multiphase machines: Part II," *IEEE Trans. Ind. Electron.*, vol. 63, no. 1, pp. 459–468, 2016.

[3] E. Levi, "Advances in converter control and innovative exploitation of additional degrees of freedom for multiphase machines," *IEEE Trans. Ind. Electron.*, vol. 63, no. 1, pp. 433–448, 2016.

[4] I. Zoric, M. Jones, and E. Levi, "Arbitrary power sharing among three-phase winding sets of multiphase machines," *IEEE Trans. Ind. Electron.*, vol. 65, no. 2, pp. 1128–1139, 2018.

[5] C. Lim, E. Levi, M. Jones, N. Rahim, and W. P. Hew, "FCS-MPC based current control of a five-phase induction motor and its comparison with PI-PWM control," *IEEE Trans. Ind. Electron.*, vol. 61, no. 1, pp. 149–163, 2014.

[6] J. A. Riveros, F. Barrero, E. Levi, M. J. Duran, S. Toral, and M. Jones, "Variable-speed five-phase induction motor drive based on predictive torque control," *IEEE Trans. Ind. Electron.*, vol. 60, no. 8, pp. 2957–2968, 2013.

[7] J. Rodas, F. Barrero, M. R. Arahal, C. Martín, and R. Gregor, "Online estimation of rotor variables in predictive current controllers: a case study using five-phase induction machines," *IEEE Trans. Ind. Electron.*, vol. 63, no. 9, pp. 5348–5356, 2016.

[8] J. Rodas, C. Martín, M. R. Arahal, F. Barrero, and R. Gregor, "Influence of covariance-based ALS methods in the performance of predictive controllers with rotor current estimation," *IEEE Trans. Ind. Electron.*, vol. 64, no. 4, pp. 2602–2607, 2017.

[9] A. Taheri, A. Rahmati, and S. Kaboli, "Efficiency improvement in DTC of six-phase induction machine by adaptive gradient descent of flux," *IEEE Trans. Power Electron.*, vol. 27, no. 3, pp. 1552–1562, 2012.

[10] A. G. Yepes, J. Malvar, A. Vidal, O. López, and J. Doval-Gandoy, "Current harmonics compensation based on multiresonant control in synchronous frames for symmetrical n-phase machines," *IEEE Trans. Ind. Electron.*, vol. 62, no. 5, pp. 2708–2720, 2015.

[11] R. Gregor and J. Rodas, "Speed sensorless control of dual three-phase induction machine based on a Luenberger observer for rotor current estimation," in *Proc. IECON*, pp. 3653–3658, 2012.

[12] M. Ayala, O. Gonzalez, J. Rodas, R. Gregor, and J. Doval-Gandoy, "A speed-sensorless predictive current control of multiphase induction machines using a Kalman filter for rotor current estimator," in *Proc. ESARS-ITEC*, pp. 1–6, 2016.

[13] H. Guzman, M. J. Duran, F. Barrero, L. Zarri, B. Bogado, I. G. Prieto, and M. R. Arahal, "Comparative study of predictive and resonant controllers in fault-tolerant five-phase induction motor drives," *IEEE Trans. Ind. Electron.*, vol. 63, no. 1, pp. 606–617, 2016.

[14] M. Bermudez, I. Gonzalez-Prieto, F. Barrero, H. Guzman, M. J. Duran, and X. Kestelyn, "Open-phase fault-tolerant direct torque control technique for five-phase induction motor drives," *IEEE Trans. Ind. Electron.*, vol. 64, no. 2, pp. 902–911, 2017.

[15] F. Baneira, J. Doval-Gandoy, A. G. Yepes, O. López, and D. Pérez-Estévez, "Control strategy for multiphase drives with minimum losses in the full torque operation range under single open-phase fault," *IEEE Trans. Power Electron.*, vol. 32, no. 8, pp. 6275–6285, 2017.

[16] J. Rodas, H. Guzman, R. Gregor, and B. Barrero, "Model predictive current controller using Kalman filter for fault-tolerant five-phase wind energy conversion systems," in *Proc. PEDG*, pp. 1–6, 2016.

[17] M. A. Fnaiech, F. Betin, G.-A. Capolino, and F. Fnaiech, "Fuzzy logic and sliding-mode controls applied to six-phase induction machine with open phases," *IEEE Trans. Ind. Electron.*, vol. 57, no. 1, pp. 354–364, 2010.

[18] Y. Kali, J. Rodas, M. Saad, R. Gregor, K. Bejelloun, and J. Doval-Gandoy, "Current control based on super-twisting algorithm with time delay estimation for a five-phase induction motor drive," in *Proc. IEMDC*, pp. 1–8, 2017.

[19] Y. Kali, J. Rodas, M. Saad, R. Gregor, K. Bejelloun, J. Doval-Gandoy, and G. Goodwin, "Speed control of a five-phase induction motor drive using modified super-twisting algorithm," in *Proc. SPEEDAM*, pp. 938–943, 2018.

[20] M. Ayala, O. Gonzalez, J. Rodas, R. Gregor, Y. Kali, and P. Wheeler, "Comparative study of non-linear controllers applied to a six-phase induction machine," in *Proc. ESARS-ITEC*, pp. 1–6, 2018.

[21] V. Utkin, J. Guldner, and J. Shi, *Sliding mode control in electromechanical systems*. Taylor-Francis, 1999.

[22] L. Fridman, "An averaging approach to chattering," *IEEE Trans. Autom. Control*, vol. 46, pp. 1260–1265, 2001.

[23] I. Boiko and L. Fridman, "Analysis of chattering in continuous sliding-mode controllers," *IEEE Trans. Autom. Control*, vol. 50, pp. 1442–1446, 2005.

[24] K. D. Young, V. I. Utkin, and U. Ozguner, "A control engineer's guide to sliding mode control," *IEEE Trans. Control Syst. Technol.*, vol. 7, no. 3, pp. 328–342, 1999.

[25] S. Drakunov and V. Utkin, "Sliding mode observers. tutorial," in *Proc. CDC*, vol. 4, pp. 3376–3378, 1995.

[26] X.-G. Yan and C. Edwards, "Nonlinear robust fault reconstruction and estimation using a sliding mode observer," *Automatica*, vol. 43, no. 9, pp. 1605 – 1614, 2007.

[27] A. Levant, "Higher-order sliding modes, differentiation and output-feedback control," *Int. J. Contr.*, vol. 76, no. 9-10, pp. 924–941, 2003.

[28] Y. Kali, M. Saad, K. Benjelloun, and A. Fatemi, "Discrete-time second order sliding mode with time delay control for uncertain robot manipulators," *Rob. Auton. Syst.*, vol. 94, pp. 53 – 60, 2017.

[29] Y. Kali, M. Saad, K. Benjelloun, and C. Khairallah, "Super-twisting algorithm with time delay estimation for uncertain robot manipulators," *Nonlinear Dynamics*, Mar 2018.

[30] Y. Kali, M. Saad, K. Benjelloun, and M. Benbrahim, "Sliding mode with time delay control for MIMO nonlinear systems with unknown dynamics," in *Proc. RASM*, pp. 1–6, 2015.

[31] Y. Kali, M. Saad, K. Benjelloun, and M. Benbrahim, *Sliding Mode with Time Delay Control for Robot Manipulators*, pp. 135–156. Singapore: Springer Singapore, 2017.

[32] V. Bandal, B. Bandyopadhyay, and A. M. Kulkarni, "Design of power system stabilizer using power rate reaching law based sliding mode control technique," in *Proc. IPEC*, pp. 923–928, 2005.

[33] J. H. Jung, P. H. Chang, and S. H. Kang, "Stability analysis of discrete time delay control for nonlinear systems," in *Proc. ACC*, pp. 5995–6002, 2007.

[34] S. Qu, X. Xia, and J. Zhang, "Dynamics of discrete-time sliding-mode-control uncertain systems with a disturbance compensator," *IEEE Trans. Ind. Electron.*, vol. 61, no. 7, pp. 3502–3510, 2014.